HHS Public Access

Author manuscript

Health Phys. Author manuscript; available in PMC 2024 October 01.

Published in final edited form as:

Health Phys. 2023 October 01; 125(4): 281–288. doi:10.1097/HP.0000000000001718.

Shielding Analysis of a Preclinical Bremsstrahlung X-ray FLASH Radiotherapy System within a Clinical Radiation Therapy Vault

Andrew Rosenstrom[1,2], **Mario Santana Leitner**[2], **Sayed Rokni**[2], **Muhammad Shumail**[3], **Sami Tantawi**[3], **John Kwofie**[4], **Shaheen Dewji**[1], **Billy W. Loo Jr.**[5]

[1] Nuclear & Radiological Engineering & Medical Physics Programs Georgia Institute of Technology, North Ave NW, Atlanta, GA 30332

[2] Radiation Protection Department, SLAC, MS 48, 2575 Sand Hill Road, Menlo Park, CA 94025

[3] Technology Innovation Department, SLAC, MS 48, 2575 Sand Hill Road, Menlo Park, CA 94025

[4] Occupational Health Center, Stanford University ESF-480 Oak Rd, Stanford, CA 94305

[5] Department of Radiation Oncology and Stanford Cancer Institute, Stanford University School of Medicine, 875 Blake Wilbur Drive, Stanford CA 94305

Abstract

Objective: A preclinical radiotherapy system producing FLASH dose rates with 12 MV bremsstrahlung x-rays is being developed at Stanford University and SLAC National Accelerator Laboratory. Because of the high expected workload of 6800 Gy w^{-1} at the isocenter, an efficient shielding methodology is needed to protect operators and the public while the preclinical system is operated in a radiation therapy vault designed for 6 MV x-rays.

Methods: In this study, an analysis is performed to assess the shielding of the local treatment head and radiation vault using the Monte Carlo code FLUKA and the empirical methodology given in the National Council on Radiation Protection and Measurements Report 151. Two different treatment head shielding designs were created to compare single-layer and multilayer shielding methodologies using high-Z and low-Z materials.

Results: The multilayered shielding methodology produced designs with a 17% reduction in neutron fluence leaking from the treatment head compared to the single layered design of the same size, resulting in a decreased effective dose to operators and the public. The conservative assumptions used in the empirical methods can lead to over-shielding when treatment heads use polyethylene or multilayered shielding.

Conclusions: High-Z/Low-Z multilayered shielding optimized via Monte Carlo are shown to be effective in the case of treatment head shielding and provide more effective shielding design

Corresponding Author: arosenstrom@gatech.edu, 502-974-3919, no fax number.

Conflicts of Interest and Sources of Funding

Bill Loo Jr has received research support from Varian Medical Systems. BWL is a co-founder and board member of TibaRay. Sami G Tantawi is a founder and board member of TibaRay Inc.

Work supported by Department of Energy contract DE-AC02-76SF00515, National Cancer Institute grant 1P01CA244091-01, Georgia Institute of Technology via subaward by SLAC under Prime Grant Project GR00014032 Award GR00014032.

For the remaining authors, no conflicts of interest or sources of funding are declared.

for external beam radiotherapy systems that use 12 MV bremsstrahlung photons. Modifications to empirical methods used in the assessment of MV radiotherapy systems may be warranted to capture the effects of polyethylene in treatment head shielding.

Keywords

Radiation Protection; Monte Carlo; Radiation Therapy; Shielding

INTRODUCTION

The development of preclinical systems that can be used in ultra-high dose rate radiation therapy is being pursued because of mounting preclinical evidence that the so-called “FLASH” effect can produce an improved therapeutic index compared to dose rates conventionally used in clinical radiation therapy (Favaudon et al. 2014, Esplen et al. 2020, Griffin et al. 2020). While promising, there is still a need for the development of preclinical systems to study the hypothesized underlying physical and biological mechanisms of FLASH radiation therapy with clinically relevant characteristics in anticipation of clinical translation (Esplen et al. 2020).

To address the need for FLASH capable preclinical systems, the FLASH experimental x-ray small animal conformal therapy (FLASH-EXACT) system is being developed at Stanford University in association with the Radiation Physics group and Technology Innovation Department at SLAC (Tantawi et al. 2020). The FLASH-EXACT device is an advanced high power (12.72 kW average beam power) linear accelerator-based radiotherapy tool designed to deliver dose at a high rate to study the biological effects of experimental FLASH radiotherapy treatments using MV energy photons. The advantage of using MV-energy photon beams is the ability to operate with clinically relevant beam energies and to be able to produce and study highly conformal dose distributions necessary for modern clinical treatments.

This work describes a novel application of the multilayered shielding method (Rosenstrom et al. 2023, Muhammad et al. 2019, Hadad et al. 2016, Cai et al. 2018) in the local treatment head shielding enabling the FLASH-EXACT device to be efficiently shielded such that it may be safely housed a clinical vault in the Stanford Cancer Center, originally designed for a 6 MV CyberKnife machine (referred to as CK-1). We examine two shielding solutions, one using methods reportedly used in some commercial machines (NCRP 1984) and a new application of the multilayered shielding methodology that uses alternating layers of high-Z and low-Z materials in the treatment head shielding to mitigate radiation more efficiently (Rosenstrom et al. 2023).

Additionally, we demonstrate the conservative nature of the methodology reported in the National Council on Radiation Protection and Measurement (NCRP) Report 151 that is commonly used in the design and assessment of MV-energy radiotherapy system shielding, particularly in the assessment of mazes in radiation vaults. We propose that a modification of this method should be made in order to assess MV-energy treatment head shielding that incorporates single layers of high-Z and low-Z materials and alternating high-Z and low-Z materials to optimize shielding of radiotherapy systems and the implied expense.

MATERIALS AND METHODS

Design of local collimator shielding

Due to the high workload, substantial secondary radiation is generated from a variety of sources, including bremsstrahlung photons, capture gamma rays, and photoneutrons during the operation of MV-energy photon radiotherapy machines. To simultaneously shield secondary radiation as well as collimate the photon beam, a treatment head shield encases the tungsten bremsstrahlung converter and the conical photon collimators. Two designs were generated for the treatment head shielding employing different layering methodologies: the so-called “single layer” and “multilayered” methodologies, which utilize a single layer or multiple alternating layers of high-Z and low-Z materials, respectively. Both designs use the same total thickness of material: 5.8 cm of tungsten, 7.7 cm of lead, and 10 cm of polyethylene. The single layer and multilayer local collimator shielding designs are represented in Figure 1; additionally, a shielding design which also uses only the high-Z material from the single layer design is used for reference to illustrate the effect that polyethylene has on radiation leaking from the collimator head.

Analysis methods

In order to simulate the radiation produced during operation, the Monte Carlo code FLUKA v2021.2 was employed to model the treatment head and shielding design (Bohlen et al. 2014, Ferrari et al. 2005). Using schematics of the CK-1 vault and linear accelerator, detailed models were implemented into FLUKA to ensure high fidelity radiation transport simulations. An implementation of the CK-1 vault in FLUKA can be seen in Figure 2; the FLUKA simulations include a high-fidelity representation of the waveguide penetration (20 cm wide × 13.5 cm high) that will provide RF power to the linac and secondary operational penetration (radius = 10.16 cm). The fluence and energy spectra of photons and neutrons, as well as the effective dose rate, were scored in FLUKA to assess the shielding performance. The effective dose rate for all particles, photons, and neutrons were scored using dose coefficients reported by ICRP Publication 74 (ICRP 1996).

With respect to particle transport, electrons were biased to preferentially undergo photon interactions using the EMF-BIAS card. Photonuclear reactions were turned on for all materials using the PHOTONUC card. The production and transport thresholds for electrons and photons were 100 keV and 50 keV respectively. Neutrons were transported to 10^{-5} eV by using the LOW-NEUT card and 260 group wise cross-sections. Region importance biasing was used to decrease the computation time to reach convergence of the effective dose rate scoring.

Empirical calculations using the methodology reported in NCRP Report 151 were used for the comparison with the FLUKA simulation results for the single-layer design (NCRP 2015). The analysis assumed a 12 MeV electron beam with a workload of 6800 Gy w^{-1}. The field size used was conservatively set to 0.36 cm^2 at the isocenter, which is 12 cm from the bremsstrahlung converter. For conventional dose rate accelerators, the largest field size, is conservative; however, this is not the case for this preclinical application, which will utilize very small field sizes resulting in a reduced dose rate at the isocenter and higher beam

losses compared to large field sizes. While larger field sizes do lead to increased leakage per electron, mainly due to the increased size of the primary beam, the cumulative effect is less than in the case of smaller field sizes in which a larger integral charge of electrons from the accelerator are required to generate the same workload. Approximately a factor of 2 more charge is needed to generate 6800 Gy/w for 0.36 cm^2 compared to 1 cm^2, due to fewer photons reaching the isocenter per electron from the increased collimation of the photon field. (Rosenstrom et al. 2021).

The assessment of Point 1 in Figure 2, located outside of the maze door, poses a challenge to the NCRP Report 151 methodology due to the specific geometry of the CK-1 vault door and door frame. An assessment of the maze and shielded door was performed using four methods: 1) Kersey Method (KM), Eq. 2.18 (NCRP 2015), to determine the neutron dose just inside of the maze door and the transmission factor provided by the maze door taken from the FLUKA simulation. 2) Modified Kersey Method (MKM), Eq. 2.19 (NCRP 2015) to determine the neutron dose just inside of the maze door and the transmission factor provided by the maze door taken from the FLUKA simulation. 3) Modified Kersey Method to determine the neutron dose just inside of the maze door followed by an empirical calculation of transmission through the maze door, shown in Eq 1. 4) Modified Kersey Method with neutron fluence at the maze entrance and maze door transmission factor from FLUKA. The different empirical analyses for the maze door are summarized in Table 1.

The equation derived following empirical relationships in NCRP 151 (NCRP 2015) and used for the empirical calculation of transmission through the maze door is given in Eq 1.

$$H_o = H_{n/p} \times W \times \frac{\sum \beta_i \times S_i}{S_t} \times 10^{\frac{-d_1}{TVD}} \quad (1)$$

Where:

H_o: neutron or photon effective dose outside of the maze door [mSv w^{-1}]

$H_{n/p}$: neutron or photon effective dose inside of the maze door [mSv Gy^{-1}]. Neutron and capture gamma effective dose rate were calculated using Eq. 2.19 and Eq. 2.15 of NCRP Report 151 (2015), respectively.

W: workload [6800Gy w^{-1}]

β_i : photon or neutron transmission factor through a particular section (i) of the maze door geometry. Transmission factors were calculated using values from NCRP Report 79 (1984) and Report 151 (2015)

S_i : surface area for a particular section (i) of the door geometry [m^2]

S_t : Total surface area of the door geometry [m^2]

d_1: distance from inside of the maze to 30cm outside of the maze door [m^2]

TVD: tenth value distance of the maze passage[m^2]

By design, the FLASH-EXACT device will always direct the primary beam toward the floor; as the CK-1 vault is located on ground level, the only components that contribute to the effective dose are patient scatter, leakage, and neutron dose. The patient scatter dose, and leakage dose was calculated using Eq. 2.7 and Eq. 2.8 from NCRP Report 151 (NCRP 2015), respectively. The neutron dose was calculated using Eq. 6.27 of *Radiation Shielding* (Shultis 2000) and dose conversion factors from NCRP Report 79 (NCRP 1984). Assessment points are shown in Figure 2 and Table 2.

Stanford Health Care follows the radiation protection requirements set by the NCRP Report 151 (NCRP 2015), which sets an effective dose rate limit of 0.1 mSv w^{-1} or 5 mSv y^{-1} for Controlled Radiation Areas and a limit of 0.02 mSv w^{-1} or 1 mSv y^{-1} for Uncontrolled Radiation Areas. The classification of the areas of interest are denoted in Figure 2 and Table 2.

RESULTS

Planar and elevation views along the highest dose rate slices for the single-layer design are shown in Figure 3. Outside of the shielded door, the effective dose rate for the single-layer and multilayer collimator design was estimated to be 0.059 mSv w^{-1} and 0.048 mSv w^{-1}, respectively, with an uncertainty of <1%. A summary of the dose rates at the points of interest are given in Table 3. In all cases, the multilayered design resulted in lower effective dose rates by ~20%, when compared to the single-layer design while occupying the same volume. This agrees with previous results reported by Rosenstrom et al. in which the multilayered shielding design proved to be more efficient (Rosenstrom et al. 2023).

Generally, the FLUKA results yield lower estimates of the effective dose rate by a factor of two to three times, compared to those produced by the NCRP Report 151 methodology. The case in which the FLUKA result is more conservative is the public sitting (Point 3). The NCRP 151 empirical method looks at the radiation streaming through the direct path between the isocenter and the point of interest; however, in this case the dose rate is underestimated due to leakage that is coming through the concrete wall in next to the machine. This wall is enclosed in the klystron house which has controlled access, but the relatively high effective dose rate in this area streams towards the Public Sitting Area. Despite this, the effective dose rate estimated using FLUKA is below the effective dose rate limit of 0.02 mSv w^{-1} without the application of an occupancy factor.

Due to the small size and solid angle of the vault penetrations in relation to the FLASH-EXACT device as well as mitigating shielding, it was found that there was negligible streaming through the three vault penetrations and that the dose rate was dominated by leakage through vault walls and the shielded door. The CK-1 vault supplemented with the treatment head adequately shields the controlled and uncontrolled radiation areas within established regulatory limits before applying the occupancy factor indicating that no further modification to the shielding design is needed.

DISCUSSION

When assessing the dose rate at Point 1, the multilayered collimator offers a 19% reduction in the effective dose rate compared to the single-layered collimator even though the same total material thicknesses were used. The main contribution to the decrease in the effective dose rate at Point 1 is the reduction in neutron fluence leaking from the treatment head due to the multilayered shielding. As shown in Figure 4, the multilayered treatment head shield results in a lower neutron fluence leaking from the treatment head at the elevation of the bremsstrahlung converter by 17%; this is the major contributing factor to the reduced dose rate outside of the maze door. The increase in the neutron fluence at the transition between lead and polyethylene is believed to be the result of neutron backscatter as neutron scattering of hydrogen results in an average scattering cosine of two-thirds. A corresponding increase in the neutron fluence is also seen in the single-layer design, and an additional bump in the neutron fluence can be seen in the second transition from lead to polyethylene in the multilayer design indicating neutron backscattering into the high-Z material. This is supported by the difference in the neutron fluence while still in the high-Z material. The bump in the neutron fluence is well defined at the boundary due to the preferential forward scattering in high-Z material. While the fluence leaking radially from the treatment head at the elevation of the bremsstrahlung converter varies, the average energy of neutrons remains constant at 51 keV and 53 keV for the single layer and multilayer designs respectively. This significantly differs from the average energy of 550 keV interpolated from Table 8 of NCRP Report 79 (NCRP 1984) i.e., when only high-Z shielding is used. This is further demonstrated in Figure 5 which contains the neutron and photon energy spectra for the single layer, multilayer, and high-Z treatment head configurations. The simulated average neutron energy when using the high-Z only treatment head is 361 keV.

The neutron fluence, as well as the average neutron energy at the isocenter, is reduced for the multilayered design; the neutron fluence is reduced by 4%; however, the fluence is two orders of magnitude higher than at the elevation of the bremsstrahlung converter. Neutrons scattering at the isocenter have a lower average energy of 349 keV for the multilayered design compared to 361 keV for the single-layer design which is equivalent to when only high-Z shielding is used. This is due to the positioning of polyethylene in relation to the distributed neutron source and the isocenter. By placing the polyethylene closer to the beamline and the isocenter, neutrons have a greater chance of passing through a moderator before scattering to the isocenter resulting in increased thermalization, however, the neutrons at the isocenter are dominated by neutrons which pass unmoderated from the bremsstrahlung converter through the photon collimator structure.

The effect of the treatment head configuration has a weaker effect on the photon leakage compared to the neutron fluence, with the photon spectra leaking from the treatment head shown in Figure 6 with the prominent gamma ray peaks being the 511 keV electron position annihilation photon and the 2041 keV gamma produced by neutron inelastic scattering with lead. The average photon energies leaking radially from the collimator head are 1173 keV, 1267 keV, and 1304 keV for the single layer, multilayer, and high-Z treatment head configurations.

The net shielding result is a 17% decrease in the neutron dose rate at the elevation of the bremsstrahlung converter and a 5% decrease in neutron dose at the isocenter. The photon fluence as well as the average photon energy did not significantly vary between designs at the elevation of the bremsstrahlung converter or the isocenter.

Due to the increased shielding performance of the multilayered treatment head, it is possible to reduce the volume and mass of shielding material while still maintaining adequate shielding performance. To demonstrate this, the multilayered design was reduced in volume in order to obtain the same shielding performance as the single-layer design resulting in potential volume and mass savings that the multilayered shielding design can provide in this application. The reduction in shielding material occurred through the removal of high-Z material or low-Z material. The mass and volume reductions achievable by removing high-Z and low-Z material are reported in Table 4. By removing polyethylene, the volume of the treatment head was reduced resulting in a so called “Multilayer - Volume Optimized” design. The neutron contribution to the effective dose rate increases in the Control Room area outside of the CK-1 vault. Similarly, removing lead resulted in a so called “Multilayer-Mass Optimized” design. The photon leakage increases from the treatment head and streams through the concrete wall directly next to the FLASH-EXACT device.

Empirical calculation using NCRP Report 151 methodology

A summary of the results of the FLUKA calculation using the single-layered and multilayered design and the NCRP Report 151 calculation for the points of interest is shown in Table 3. The NCRP calculation provides conservative estimates for all points of interest except for Point 3, as previously mentioned.

At several points when using the NCRP Report 151 methodology, values from FLUKA were needed in order to realistically capture the leakage factor, neutron source term, and average neutron energy. The need for the use of FLUKA values is derived from initial studies on which NCRP Report 151 is based, (NCRP 2015, McCall et al. 1999, Martin and McGinley 2002) which only consider head shielding that is high-Z, either tungsten, lead, or iron. This affects the assumptions of the empirical equations through the neutron and capture gamma spectrum and fluence in several ways.

First, high-Z materials have lower energy peaks in giant dipole resonances and higher cross-sections at the peak for photoneutron production resulting in a significantly higher neutron fluence per Gy at the isocenter while subsequently providing minimal attenuation of the neutron fluence. This is demonstrated in the values of 1 and 0.85 for transmission factors to be used in Eq. 2.16 of NCRP Report 151 (NCRP 2015). Second, high-Z materials do influence the neutron spectrum through the neutron separation energy ~7.3 MeV, and moderation provided by elastic and inelastic scattering reactions (NCRP 1984), but at no point is the effect of polyethylene or the multilayering of polyethylene and high-Z considered in the fluence or energy spectra of neutrons leaking from the treatment head. For that reason, the values in Table B.9 of NCRP Report 151 were not used for the neutron source term, as the Saturne-41 linear accelerator produced a neutron fluence that was two orders of magnitude higher than the neutron fluence from the FLUKA simulations (NCRP 2015).

Eq. 2.16 of NCRP report 151 was still used for the calculation of the neutron fluence at the maze entrance; however, the coefficients representing the different flux components are based on empirical measurements from machines that only use high-Z head shielding (NCRP 2015). This created large differences when the neutron effective dose rate was calculated with the MKM approach using the value of $\phi_A = 1.94 * 10^7\ m^{-2} Gy_{iso}^{-1}$ calculated from Eq. 2.16 and when it was measured in FLUKA. The effective dose rate inside of the maze door as simulated by FLUKA is 0.171 mSv w^{-1}, while the MKM approach yields 0.44 mSv w^{-1}. This difference in the neutron dose rate is driven by the neutron spectra because the neutron fluence at the maze door is reduced by only 14% from the value calculated empirically using Eq. 2.16. This is also supported by the KM approach, which is a dose-based approach rather than a fluence-based approach. As shown in Table 3 as well as in the value of 0.24 mSv w^{-1} inside of the maze door, the KM approach has better agreement indicating the effect of the neutron spectra on the neutron fluence at the maze entrance since the KM approach applies only geometric attenuation based on the maze and room dimensions.

An additional simulation was performed with only high-Z head shielding where the neutron effective dose rate value inside the maze was determined to be 0.33 mSv w^{-1}. The effective dose rate outside of the maze door at Point 1 was found to be 0.12 mSv w^{-1}. These values are more aligned with the results of the MKM approach indicating the effect of the neutron spectra is not captured by this fluence-based method.

The NCRP Report 151 estimate of the dose from photons at the inside of the maze door agrees well with the results from the FLUKA simulation. The results from the NCRP Report 151 calculation show that photons deliver 16% of the effective dose; this value has high uncertainty stemming from the albedo coefficients (± 50% uncertainty) reported in Table B8a of NCRP Report 151 (2015) of the effective dose, while the single and multilayered FLUKA simulations show 16% and 14% with uncertainties of 9.8 and 9.5 % respectively.

For these reasons, the implications of this study suggest that the NCRP Report 151 methodology can be adjusted to account for the effect of polyethylene and multilayered treatment head shielding. Improvements to the estimate of the fluence and energy spectra of neutrons and capture gammas will enable shielding design without the use of computer codes and will allow regulators to assess the effect of the treatment head shielding more accurately on radiotherapy machines so that designs are not produced with excess shielding. The authors are currently pursuing empirical methods to capture these effects.

CONCLUSION

A 12 MeV, 12.76 kW FLASH radiotherapy machine is being designed for preclinical radiotherapy experiments and will be able to deliver a highly conformal beam for clinically relevant experiments. In order to adequately shield the system, a novel application of multilayered shielding method to the collimator shielding head was performed.

Radiological analysis was performed using a well-established multi-particle radiation transport code as well as NCRP Report 151 empirical calculations, in order to assess

the impact of housing the device inside of the CK-1 vault. A high-fidelity model of the CK-1 vault was created to calculate the effective dose to operators and the public from the secondary radiation generated by the operation of the FLASH-EXACT device. Results demonstrated that effective dose rates in controlled and uncontrolled radiation areas were below the NCRP Report 151 limits without the application of occupancy factors. Additionally, evidence was presented demonstrating that modification to empirical methods used in design and regulation is advisable. If followed, the empirical methods presented in NCRP Report 79 and Report 151 would have resulted in over-shielding of the machine by as much as 1 half value layer if the Modified Kersey Method were used to assess the dose streaming through the maze.

The effect of the multilayered shielding methodology (Rosenstrom et al. 2023) was confirmed in simulations where it was applied to the treatment head shielding with a 19% reduction in the effective dose rate in the Control Room as well as reduced the effective dose rate all points of interest. Additionally, mass and volume reductions can be performed with the multilayered design resulting in small and lighter treatment head shielding. Therefore, the multilayered shielding methodology offers a path forward in the design of efficient and economic head shielding for preclinical and clinical FLASH radiotherapy machines using high-energy bremsstrahlung.

REFERENCES

Bohlen TT, Cerutti F, Chin MPW, Fasso A, Ferrari A, Ortega PG, Mairani A, Sala PR, Smirnov G, Vlachoudis V. The FLUKA Code: Developments and Challenges for High Energy and Medical Applications. Nuclear Data Sheets. 2014;120:211–214. doi:10.1016/j.nds.2014.07.049

Cai Y, Hu H, Pan Z, Hu G, Zhang T. A method to optimize the shield compact and lightweight combining the structure with components together by genetic algorithm and MCNP code. App. Rad. and Isotopes 139 p 169–174 2018. doi:10.1016/j.apradiso.2018.05.009

Esplen N, Mendonca MS, and Bazalova-Carter M, Physics and biology of ultrahigh dose-rate (FLASH) radiotherapy: a topical review, Physics in Medicine & Biology 2020;63(23). doi:10.1088/1361-6560/abaa28.

Favaudon V, Caplier L, Monceau V, Pouzoulet F, Sayarath M, Fouillade C, Poupon MF, Brito I, Hupe P, Bourhis J, Hall J, Fontaine JJ, Vozenin MC. Ultrahigh dose-rate FLASH irradiation increases the differential response between normal and tumor tissue in mice. Sci Transl Med 2014;6. doi:10.1126/scitranslmed.3008973.

Ferrari A, Sala PR, Fasso A, Ranft J. FLUKA: A multi-particle transport code (Program version 2005), (2005).

Griffin RJ, Ahmed MM, Amendola B, Belyakov O, Bentzen SM, Butterworth KT, Chang S, Coleman CN, Djonov V, Formenti SC, Glatstein E, Guha C, Kalnicki S, Le QT, Loo BW Jr, Mahadevan A, Massaccesi M, Maxim PG, Mohiuddin M, Mohiuddin M, Mayr NA, Obcemea C, Petersson K, Regine W, Roach M, Romanelli P, Simone CB 2nd, Snider JW, Spitz DR, Vikram B, Vozenin MC, Abdel-Wahab M, Welsh J, Wu X, Limoli CL. Understanding High-Dose, Ultra-High Dose Rate, and Spatially Fractionated Radiation Therapy. Int J Radiat Oncol Biol Phys. 2020 Jul 15;107(4):766–778. doi: 10.1016/j.ijrobp.2020.03.028. Epub 2020 Apr 13. PMID: 32298811. [PubMed: 32298811]

Hadad K, Nematollahi M, Sadeghpour H, Faghihi R. Moderation and shielding optimization for a 252Cf based prompt gamma neutron activation analyzer system. Int. J. of Hydrogen Energy 2016;41(17):7221–7226. doi:10.1016/j.ijhydene.2015.12.208

International Commission on Radiological Protection “Conversion Coefficients for use in Radiological Protection against External Radiation.”, ICRP (1996).

Martin M, McGinley PH. Shielding techniques for radiation oncology facilities Medical Physics (2002)

McCall RC, McGinley PH, Huffman KE. Room scattered neutrons. Med Phys. 1999 Feb;26(2):206–7. doi: 10.1118/1.598505. PMID: 10076975. [PubMed: 10076975]

Muhammad AS, Rashid NKAM, Hamzah K. A review on multilayer radiation shielding. IOP Conf. Ser.: Mater. Sci. Eng. 2019;555:012008. doi:10.1088/1757-899X/555/1/012008

National Council on Radiation Protection and Measurement “Neutron Contamination from Medical Electron Accelerators” (1984)

National Council on Radiation Protection and Measurement “Structural Shielding Design and Evaluation for Megavoltage X- and Gamma-Ray Radiotherapy Facilities”, NCRP (2015).

Rosenstrom A, Santana-Leitner M, Rokni S, Manjappa R, Graves E Loo BW Jr. “Radiation Protection Analysis for Housing the FLASH Exact Project in Stanford’s CK-1 Vault” RP-note-21–21 (2021)

Rosenstrom A, Santana-Leitner M, Rokni S, Shumail M, Tantawi S, Dewji S. Loo BW Jr. Monte Carlo simulation of shielding designs for a cabinet form factor preclinical MV-energy photon FLASH radiotherapy system Med. Phys doi:/10.1002/mp.16290 (2023)

Shultis J and Faw R Radiation Shielding American Nuclear Society United States ISBN:0–89448-456–7 (2000)

Tantawi S, Nasr M, Li Z, Limborg C, and Borchard P. Design and demonstration of a distributed-coupling linear accelerator structure. United States. 10.1103/PhysRevAccelBeams.23.092001

Vlachoudis V Flair: A powerful but user friendly graphical interface for FLUKA. (United States: American Nuclear Society - ANS, 2009).

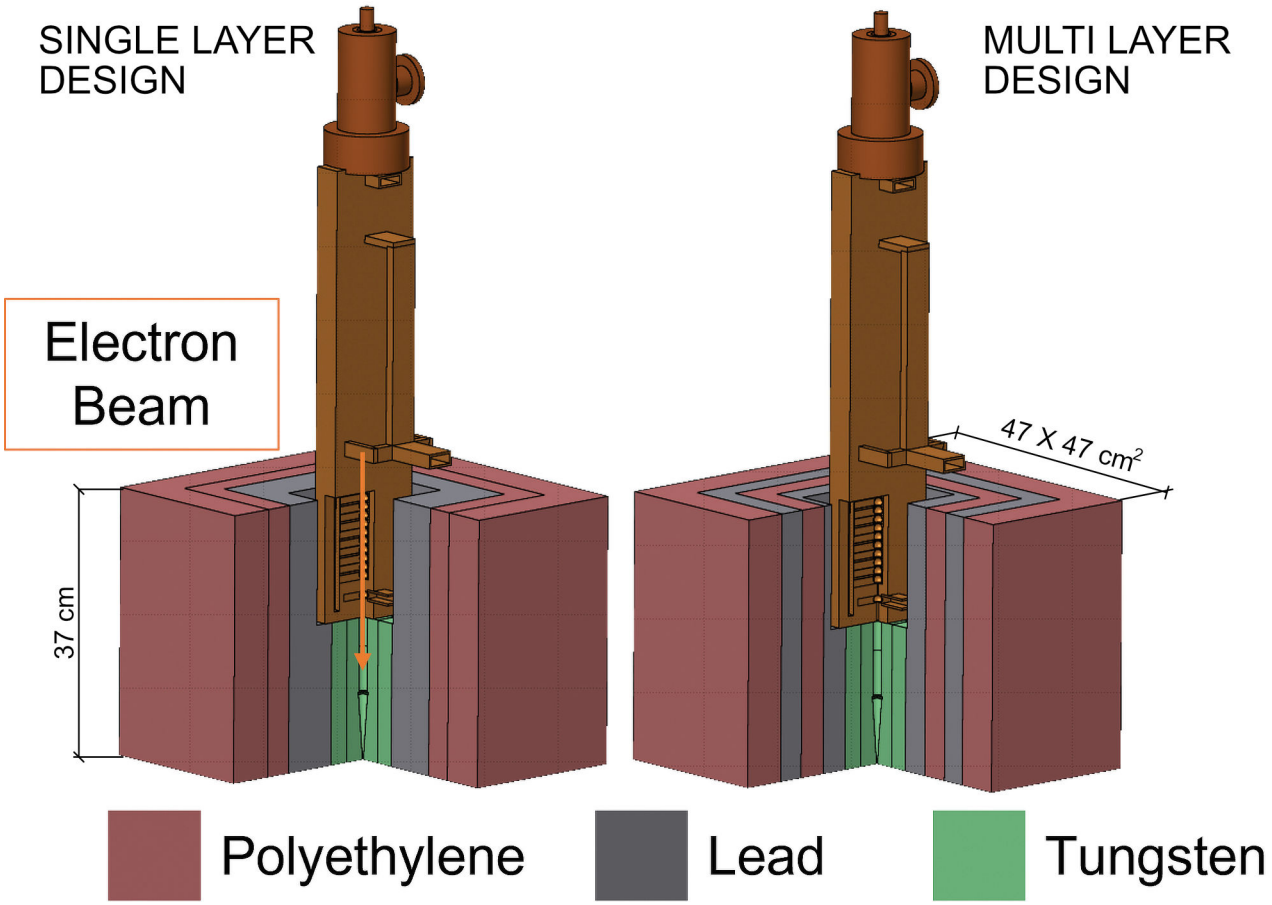

Figure 1:
3D representation of treatment head geometry used for testing in the CK-1 vault. The materials of collimator shielding are polyethylene (green), lead (dark-grey), tungsten(light-grey). Source images produced in Flair (Vlachoudis 2009). The single layer design, approximately 350 kg, stems from information documented in NCRP report 79 (NCRP 1984). The multilayered treatment head shielding design, approximately 390 kg, utilizes the same shielding methodology as reported by Rosenstrom et al (Rosenstrom et al. 2023).

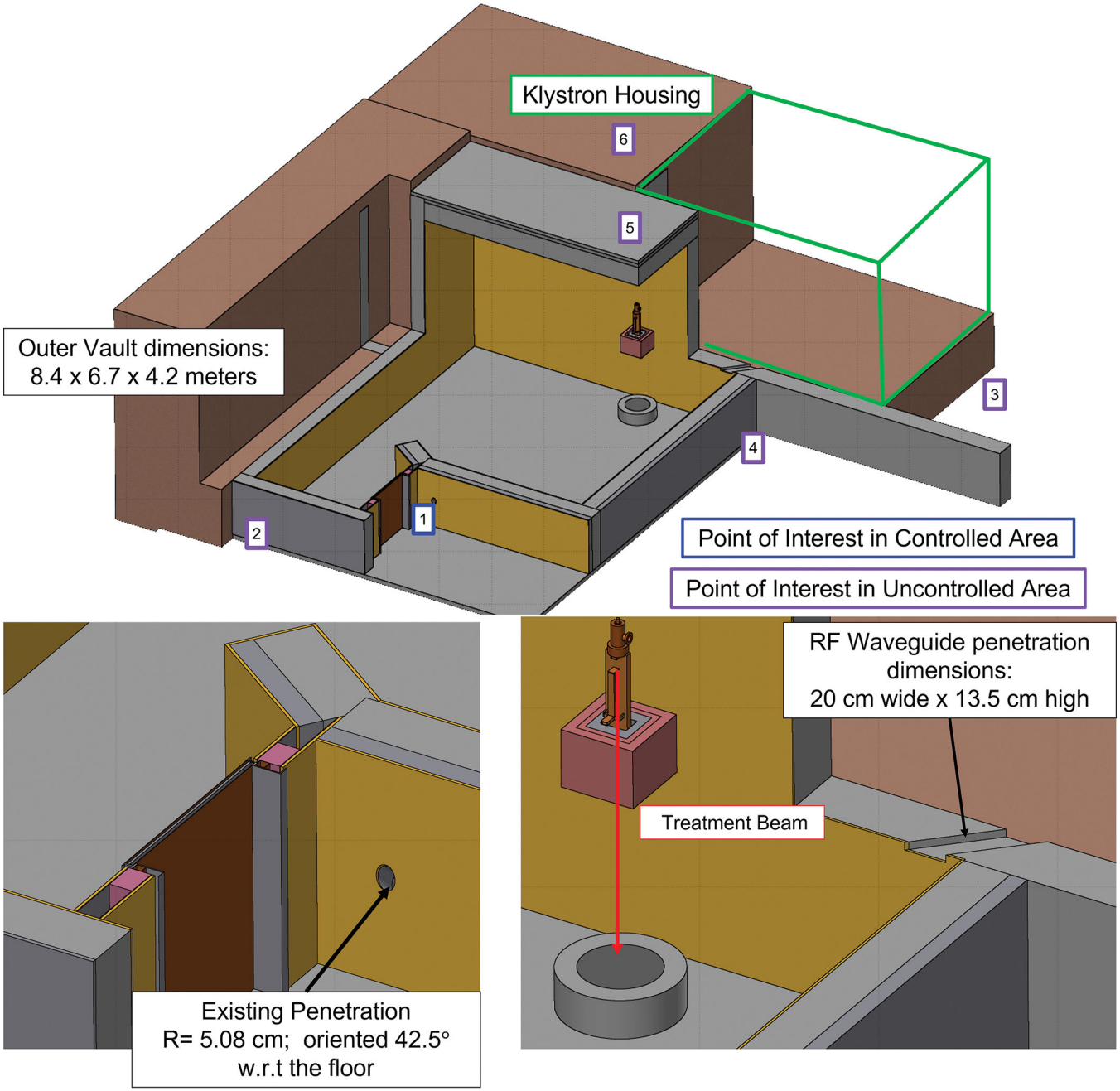

Figure 2:

3D representation of the CK-1 vault implemented in FLUKA. The geometry of the maze door, door frame and wave guide penetrations are noted. Controlled and Uncontrolled Radiation Areas are denoted in blue and purple, respectively. Points of interest for which the NCRP Report 151 calculation was performed are denoted. Further detail is provided for the points of interest in Table 2. Images produced in Flair (Vlachoudis 2009).

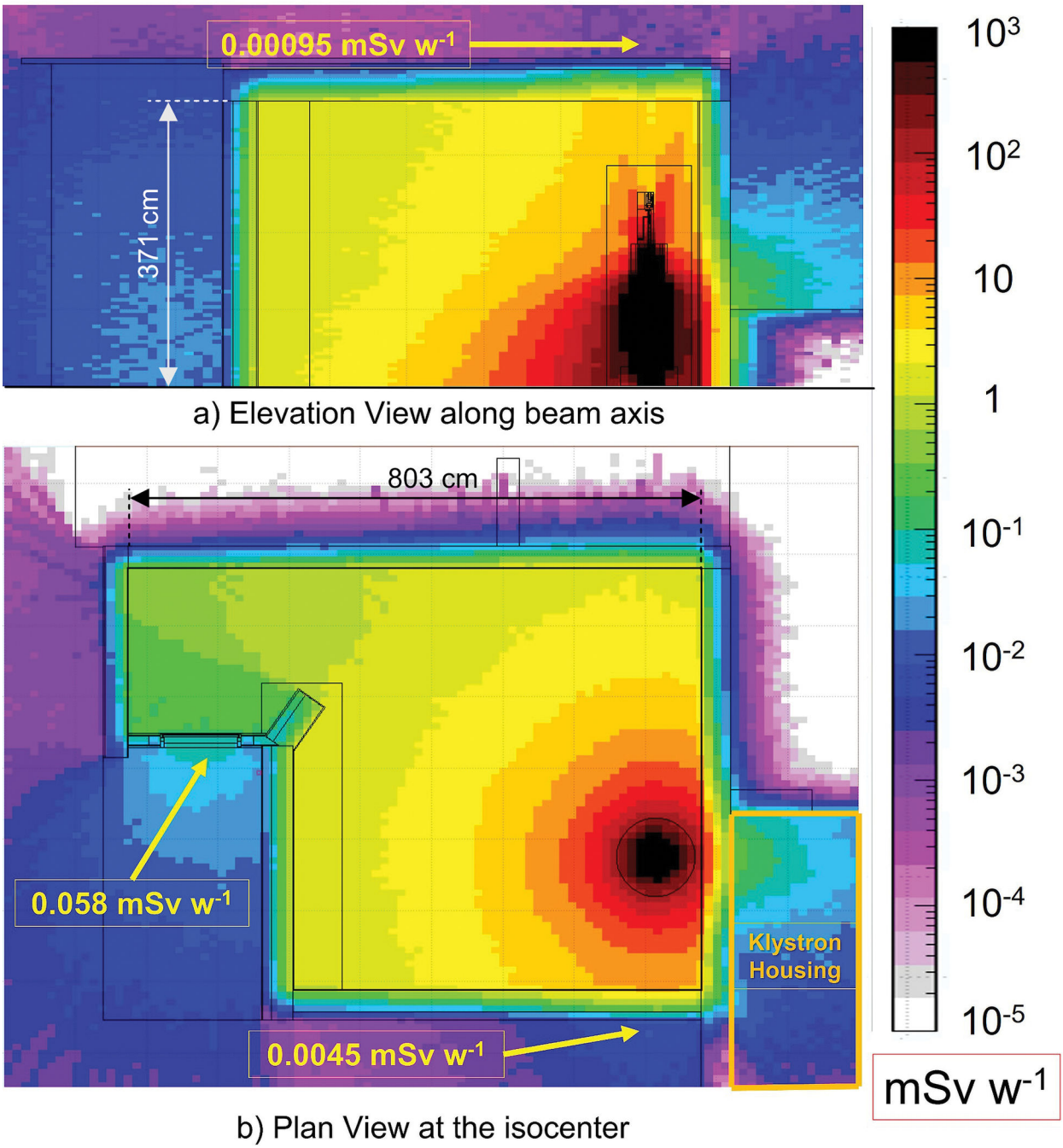

Figure 3:
Elevation view (3a) and planar (3b) effective dose rate maps of the CK-1 for 1 week of operation for the single-layer design with a workload of 6800Gy w-1. Results are reported in mSv w-1. The slice of the elevation view A' is denoted in the planar view.

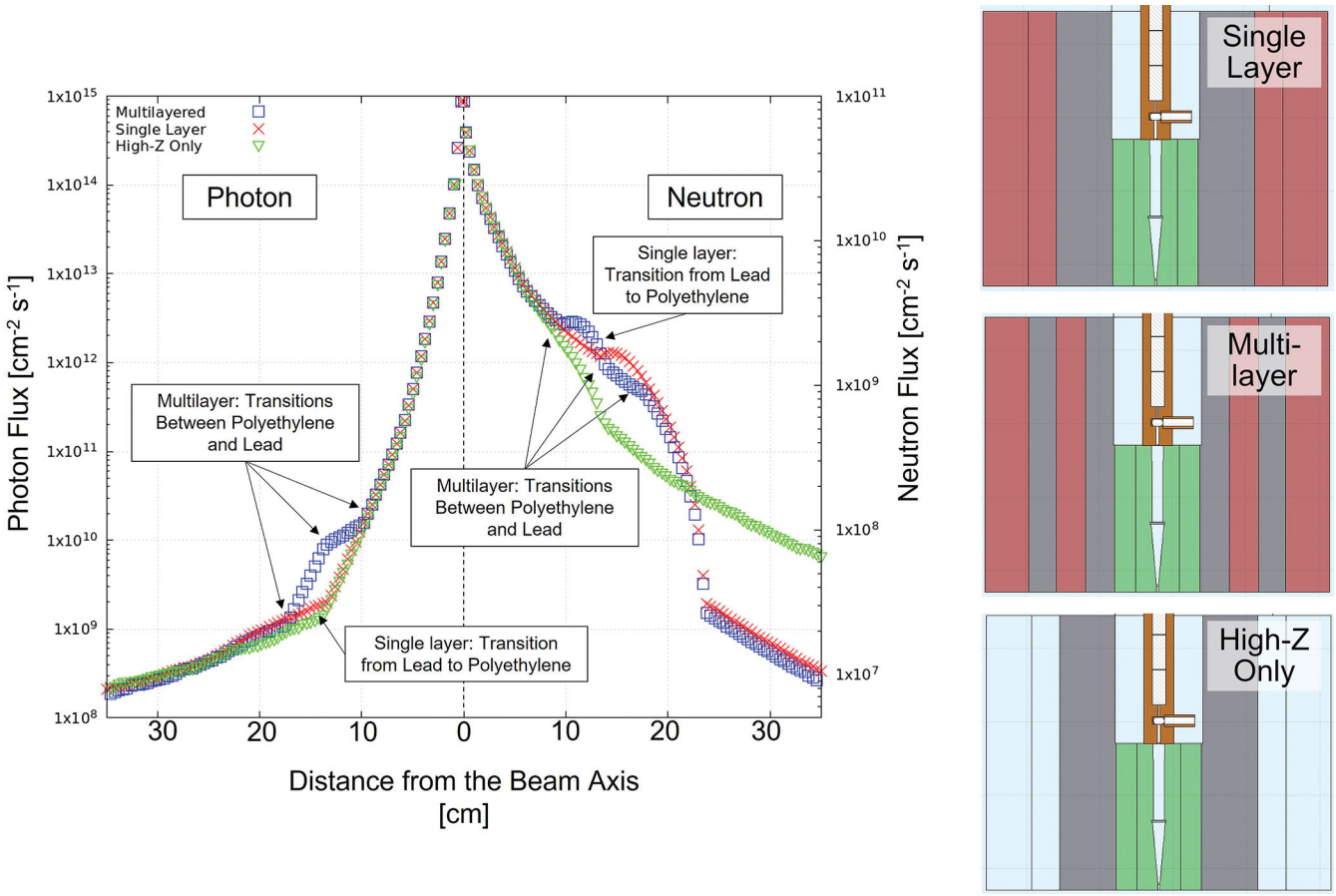

Figure 4:

Photon flux (left) and neutron flux (right) leaking through the single layer, multilayered, and high-Z-only collimator designs at the elevation of the bremsstrahlung converter. Material layers are denoted with their respective arrows. Error bars yield uncertainties less than 1%. 2-D cross-sections of the treatment head are shown for reference.

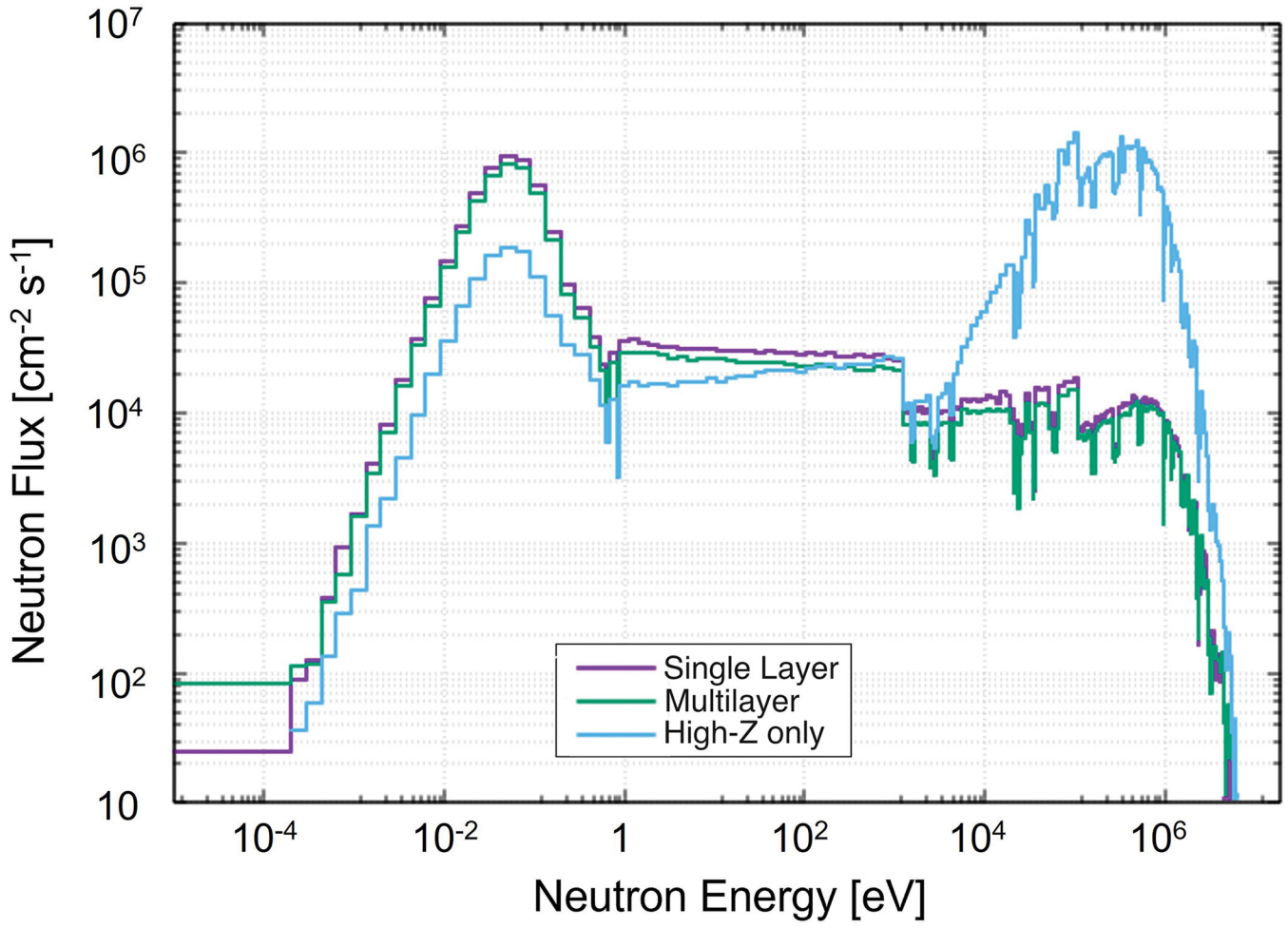

Figure 5:
Neutron energy spectrum leaking radially from the single layer, multilayer and high-z treatment head configurations.

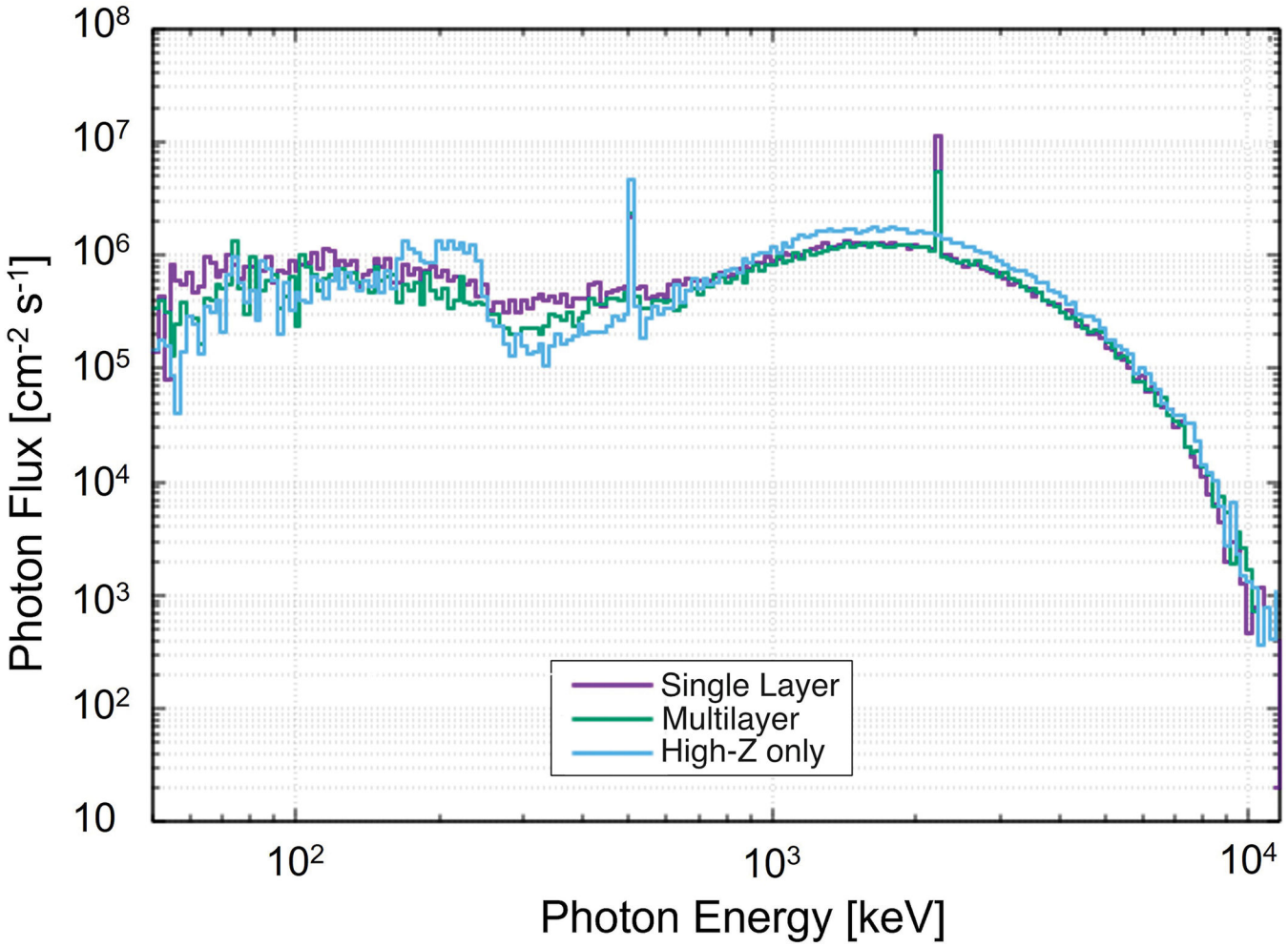

Figure 6:
Photon energy spectrum leaking radially from the single layer, multilayer and high-z treatment head configurations.

Table 1:

Summary of the empirical analyses conducted for the assessment of the neutron dose rate passing through the door

Analysis	Method	Description of Input to the Method	Source of Input	Handling of Transmission Through the Maze door
1	Kersey Method	Neutron dose at 1.41 meters	FLUKA Simulation of neutron dose at this point	Average attenuation simulated in FLUKA through the maze door
2	Modified Kersey Method	Neutron fluence at the maze entrance	Using Eq 2.16 from NCRP 151	Average attenuation simulated in FLUKA through the maze door
3			Using Eq 2.16 from NCRP 151	Using Eq 1
4			FLUKA simulation of the neutron fluence at the maze entrance	Average attenuation simulated in FLUKA through the maze door

Table 2:

Summary of the points of interest used in the analysis using the NCRP Report 151 methodology; Depictions of the points of interest relative to the FLASH EXACT device are shown in Figure 2. Distances to the points of interest are 30 centimeters from the shielding boundary.

Position	Description	Distance from isocenter (m)	Concrete Thickness (cm)	Lead Thickness (cm)	Area Type	Occupancy Factor (NCRP 2015)
1	Control Room	5.99	30	12	Controlled	1
2	Mechanical Room	9.04	28	2.79	Uncontrolled	0.05
3	Public Sitting Area	6.65	113	0.0	Uncontrolled	0.05
4	Office Space	2.54	30	12	Uncontrolled	1
5	Office Space 1st Floor	3.09	48.3	7.62	Uncontrolled	1
6	Garden Area	3.75	85	0.0	Uncontrolled	0.025

Table 3:

Total effective dose rate at the points of interest and comparison to FLUKA calculations for single layer and multilayered collimator designs, occupancy factors were not included.

Position	NCRP Report 151 Calculation (mSv w^{-1})	FLUKA Calculation (Single Layer) (mSv w^{-1})	FLUKA calculation (Multilayer) (mSv w^{-1})
Control Room (KM w/Attenuation Factor from FLUKA)	9.1×10^{-2}	5.90×10^{-2}	4.84×10^{-2}
Control Room (MKM w/Attenuation Factor from FLUKA)	1.6×10^{-1}		
Control Room (MKM w/ Eq 1)	2.0×10^{-1}		
Control Room (MKM w/ Attenuation Factor and ϕ_A from FLUKA)	1.3×10^{-1}		
Mechanical Room	8.3×10^{-3}	1.36×10^{-3}	1.21×10^{-3}
Public Sitting Area	1.0×10^{-4}	4.04×10^{-4}	2.03×10^{-4}
Office Space	4.8×10^{-2}	4.47×10^{-3}	1.52×10^{-3}
Office Space 1st Floor	4.6×10^{-2}	1.50×10^{-3}	9.54×10^{-4}
Garden Area	1.1×10^{-4}	1.96×10^{-5}	1.02×10^{-5}

Table 4:

Summary of potential volume and mass reductions possible when using the multilayered treatment head design while maintaining shielding performance compared to the single-layer design.

Treatment Head Shielding Design	Total Thickness of Lead (cm)	Total Thickness of Polyethylene (cm)	Mass of Shielding (kg)	Volume of Shielding (cm3)	Limiting Dose Rate Location
Reference Single Layer	7.7	10	350	57,085	N/A
Reference Multilayer	7.7	10	390	57,085	N/A
Multilayer - Volume Optimized	7.7	7.5	374	44,615	Control Room
Multilayer - Mass Optimized	5.6	10	329	49,575	Public Sitting Area